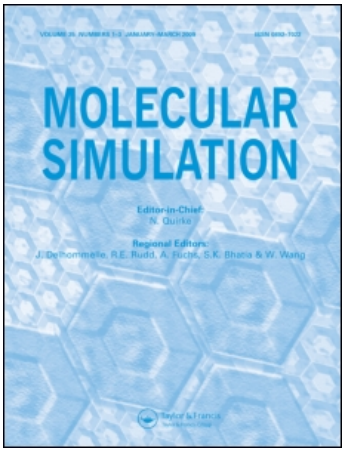


**Molecular Simulation**
Publication details, including instructions for authors and subscription information:
http://www.informaworld.com/smpp/title~content=t713644482

# First-principles investigation of the interaction of gold and palladium with armchair carbon nanotube

Francesco Buonocore[a]
[a] STMicroelectronics Srl TR&D Post Silicon Technologies, Arzano Naples, Italy

Online publication date: 15 October 2010

**To cite this Article** Buonocore, Francesco(2010) 'First-principles investigation of the interaction of gold and palladium with armchair carbon nanotube', Molecular Simulation, 36: 10, 729 — 735
**To link to this Article: DOI:** 10.1080/08927021003699807
**URL:** http://dx.doi.org/10.1080/08927021003699807

*Molecular Simulation*
Vol. 36, No. 10, September 2010, 729–735

Taylor & Francis
Taylor & Francis Group

# First-principles investigation of the interaction of gold and palladium with armchair carbon nanotube

Francesco Buonocore*

*STMicroelectronics Srl TR&D Post Silicon Technologies, Via Remo de Feo, 1, 80022 Arzano Naples, Italy*

(*Received 20 October 2009; final version received 14 February 2010*)

In this paper, we investigate the adsorption mechanisms at the interface between carbon nanotubes and metal electrodes that can influence the Schottky barrier (SB). We developed a theoretical model based on the first-principles density functional theory for the interaction of an armchair single-wall carbon nanotube (SWNT) with either Au(111) or Pd(111) surface. We considered the side-wall contact by modelling the full SWNT as well as the end-contact geometry using the graphene ribbon model to mimic the contact with very large diameter nanotubes. Strong interaction has been found for the Pd–SWNT interface where the partial density of states (DOS) shows that d-orbitals of palladium are dominant at the Fermi energy so that the hybrid Pd-orbitals have the correct symmetry to overlap with $\pi$-electrons and form covalent bonds. The SWNT can only be physisorbed on the gold surface for which the contribution to the DOS of the d-orbitals is very low. Moreover, the filling of antibonding states makes the Au–SWNT bond unstable. The average and 'atom to atom' energy barriers at the interface have been evaluated. The matching of open-edge carbon dimers with metal lattice in the end-contact geometry is more likely for large diameter SWNTs and this makes lower the SB at the interface.

**Keywords:** carbon nanotube; density functional theory; adsorption; metals; interconnects



## 1. Introduction

The subject of the interaction between carbon nanotubes (CNTs) and metal surface or cluster has been gaining a growing interest in the last years. Indeed, CNTs have been proposed as innovative one-dimensional nanostructure with superior electrical properties to be employed in applications such as field-effect transistors (FETs) [1–3], field-emission displays [4] or single-electron transistors [5,6], where metal contacts can be required to integrate the carbon wires within the device.

CNT-FETs fabricated using thick-gate dielectrics and medium-to-high work function metals are mostly p-type in air, but, after annealing in vacuum, they can be converted to ambipolar and even further to n-type [7,8]. This was an indication that Schottky barrier (SB) at the metal–CNT interface dominates the transistor switching. The CNT-FET can also operate in ways similar to conventional MOSFETs (ohmic junction) [9].

Moreover, the feature sizes in Si integrated circuits are continually reducing and the interconnects between each transistor are forced to carry increasingly larger current densities. Therefore, CNTs have also been proposed [10] to be used as interconnects at the same time as CNTs can carry very high current density, before failing as a result of electromigration. Contacts with vanishing SB are essential because the overall resistance is lowered.

It was evidenced [11] that the width of the SB depends on the band gap of the CNT material (inversely proportional to the diameter) and the work function of the contacting metal. Either large diameter CNTs or metal contacts with high work function give small SBs.

It has also been observed that irregular experimental results are found for metals with high chemical reactivity (e.g. Ti) for which metal carbide at the interface can be formed after annealing [3], decrementing the quality of the contact.

The theoretical investigation based on first principles helped to improve the understanding of the mechanisms that can influence the SB at the interface between the single-wall carbon nanotube (SWNT) and metal. The authors of the first models of the contacts on the atomic scale [12,13] demonstrated that semiempirical descriptions ignoring the microscopic features of the contacts cannot suffice to fully understand the electronic structure at the small metal–SWNT junction but the detailed atomic geometries should be integrated. It was shown [13] that Au does not side-wall bind to the SWNT, differently from other metals (e.g. Mo, Pd and Pt), and this takes into account of the large SB found in experiments at the Au–SWNT interface.

The wetting of graphene surface by metal films or clusters has been investigated [14], finding that metals with smaller cohesive energy are expected to form clusters more mobile on the surface, and larger cohesive energy is expected to result in coalescence into bigger clusters and non-wetted surface. Once this is clarified, it is understood

*Email: francesco.buonocore@st.com

ISSN 0892-7022 print/ISSN 1029-0435 online

DOI: 10.1080/08927021003699807
http://www.informaworld.com

that Pt, characterised by large cohesive energy, does not create contacts as good as Pd does, despite the work function of Pt being larger.

Recently, models of SWNT fully embedded in metal have been proposed [15–17]. The inspection of the electrostatic potential in the contact region is very important in order to investigate the SB. In particular, Zhu and Kaxiras [16] investigated the electrostatic potential and found that there is no SB to electron transfer between Pd and SWNT. On the other hand, it has been demonstrated [17] that not only the chemical bond occurring at the interface plays an important role in determining the SB, but also the preservation or breaking of the $\pi$-conjugation of the SWNT should be taken into account.

In this paper, we investigate orbital overlapping between the metal surface and the SWNT hybrid orbitals by studying the partial contributions of metal and SWNT states of different angular momentum to the density of states (DOS). In this way, we describe how the bonding takes place. Indeed, the angular momentum contributing more to the DOS determines the symmetry of the hybrid orbitals. In order to have overlapping orbitals, it is important that the metal and the adsorbate hybrid orbitals have the correct symmetry, and then metal and carbon atoms can coordinate to form bonds.

We developed a model for an ideal metal–SWNT contact in the side-wall geometry by first principles. Therefore, we model a SWNT deposited above a metal substrate, Pd(111) or Au(111), free to bind with the metal. Moreover, we looked for insights also into the end-contact geometry using the graphene ribbon model in vertical contact with the metal surface to mimic the contact with very large diameter SWNTs.



## 2. Theoretical method and model

Our theoretical investigation was carried out with calculations based on the density functional theory (DFT) within the generalised gradient approximation with the Perdew, Burke and Ernzerhof correlation functional. Our calculations were performed using the DMol[3] program (Accelrys, Inc., San Diego, CA, USA) [18,19]. The electronic wave functions are expanded in atom-centred basis functions defined on a dense numerical grid. The chosen basis set was double numerical plus polarisation where each basis function was restricted to a global cut-off radius of 4.5 Å. The chosen cut-off value leads to atomic energies with an accuracy of 0.1 eV/atom, allowing calculations without significant loss of accuracy. The core electrons of the metals were described using DFT semi-core pseudopotentials (DSPPs) [20] that replace core electrons by a single effective potential, reducing the computational cost. DSPPs introduce some degree of relativistic correction into the core.

All geometry optimisations were performed using a scheme based on delocalised internal coordinates generalised to periodic boundary conditions. The Brillouin-zone integrations were performed using a $3 \times 1 \times 1$ Monkhorst–Pack grid for the metal–SWNT systems and a $6 \times 5 \times 1$ Monkhorst–Pack grid for the metal–carbon ribbon systems.

We have modelled an armchair (5,5) SWNT with a diameter of 6.9 Å either physisorbed or chemisorbed by the side wall to the gold or platinum electrode, respectively. The metal surfaces have been modelled by the repeated slab geometry which contains three atomic layers, with the atomic coordinates of the lowest layer constrained. The comparison with the five layer slabs shows a gain of the total energy of 0.12 eV/atom and a shift of the Fermi level (measured with respect to the vacuum level) of 0.03 eV for both Au and Pd systems. Therefore, our model is sufficiently accurate to describe the electron hybridisation at the interface.

The geometry-optimised structures are illustrated in Figure 1. The edges of the periodic cell are $a = 4.995$ Å, $b = 14.420$ Å and $c = 25.0$ Å for the Au(111)–SWNT model, and $a = 4.765$ Å, $b = 11.005$ Å and $c = 25.0$ Å for the interface with Pd. The lattice parameter $c$ is chosen in the direction normal to the (111) plane along the $z$-axis, while $a$ and $b$ are along the $x$- and $y$-axes, respectively. The width of $c$ is such that the interactions among the periodic images of the system are negligible in the $z$-direction. The lattice parameter of the SWNT along its axis has been expanded (compressed) by 2.3% to match the surface periodicity of the Au (Pd) slab.

## 3. Results and discussion

We present our results on the electronic structure and the self-consistent-field (SCF) electrostatic potential of the interfaces between the SWNT and the metal slabs.

The binding energy of the Au(111)–SWNT system is 0.70 eV and the SWNT–slab distance was initially set to 2.3 Å, but it increased to 3.6 Å as a result of full-structure optimisation. The plane-averaged electrostatic energy of the system has been calculated and is reported in Figure 2. In this paper, we define the average energy barrier as the difference between the maximum of the average electrostatic energy in the metal–SWNT interface region and the Fermi energy, as illustrated in Figure 2. The Fermi energy $E_F$ is defined from the condition $\int_{-\infty}^{E_F} \mathrm{DOS}(E)\mathrm{d}E = N$, where DOS($E$) is the DOS of the full system and $N$ is the total number of electrons. The average energy barrier resulted to be 6.0 eV for Au. We have also calculated the SCF electrostatic potential in a plane containing the two nearest C and Au atoms with a distance of 3.685 Å. The energy barrier that an electron has to overcome along the shorter path between Au and C is 4.31 eV, and we call this as the 'atom to atom' energy barrier.

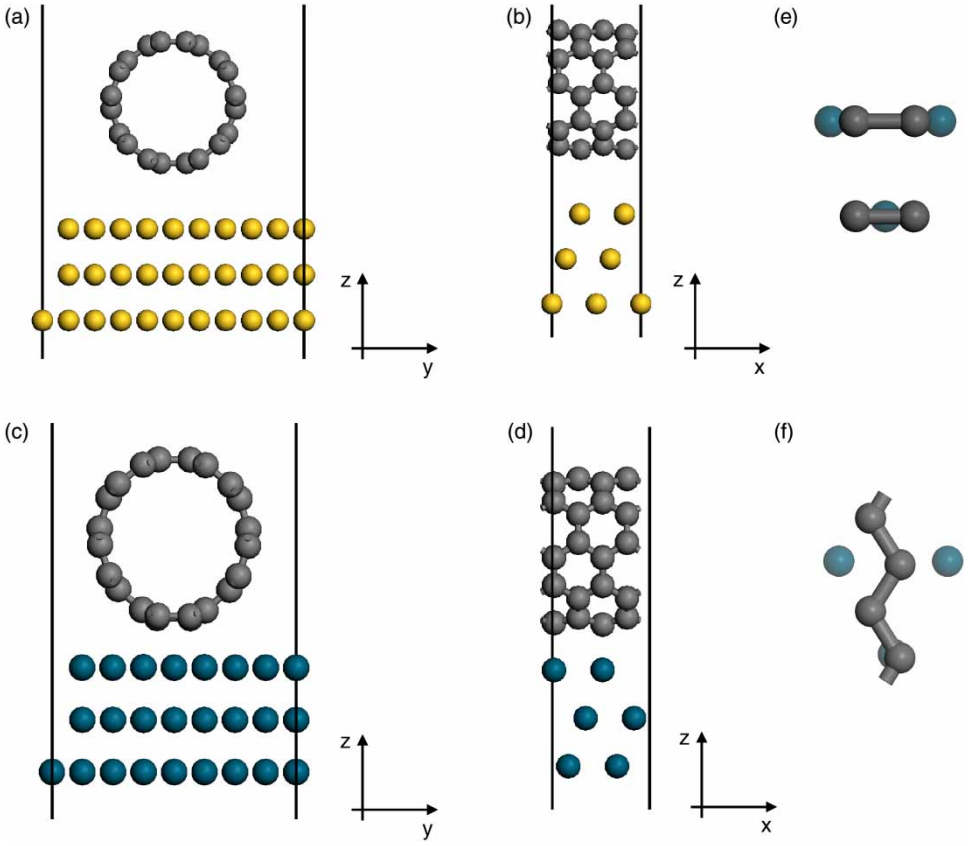


Figure 1. Atomistic periodic model after optimisation of the interface of the gold slab with the SWNT in (a) front view and (b) side view. The same is shown for the palladium slab as (c) front view and (d) side view. Also, the views normal to the (111) plane of the nearest carbon and palladium atoms within the periodic cell for (e) chemisorbed and (f) physisorbed SWNT are shown.



The same calculations were done for the Pd(111)–SWNT system. The binding energy is 1.30 eV and the SWNT–slab distance is 2.22 Å after geometry optimisation. The binding energy is defined as $E$(SWNT–Metal)–$E$(SWNT)–$E$(Metal), where $E$(SWNT–Metal) is the total energy of the relaxed full system and $E$(SWNT) ($E$(Metal)) is the total energy of the isolated SWNT (metal slab) in the same relaxed geometry and unit cell of the full system. The average energy barrier at the interface with the SWNT was evaluated to be 2.4 eV but the SCF electrostatic potential, mapped in Figure 3(a), along the Pd—C bond of length 2.30 Å shows that no 'atom to atom' energy barrier is found. While the average electrostatic potential seems to hinder the charge transfer from the electrode, local paths do exist where charges can be freely transferred. The measured SB is probably not straightly the average energy barrier but something of the intermediate between the average and 'atom to atom' energy barriers. For example, an experimental value of the Pd–SWNT SB for the selected diameter is 0.4 eV [11].

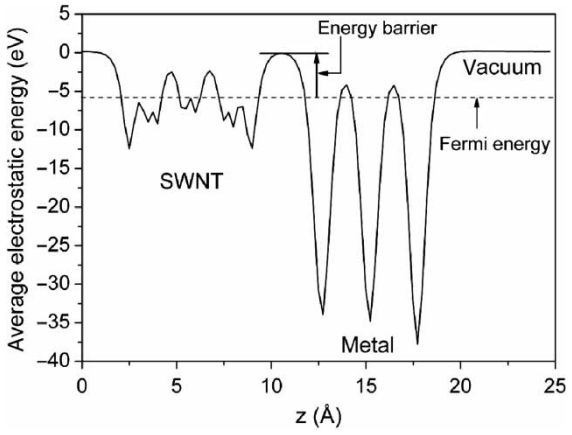


Figure 2. Plane-averaged electrostatic energy of the Au(111) slab with adsorbed SWNT.

A covalent bond is formed at the interface with Pd, and it can be seen from the calculation of a positive charge density difference, mapped in Figure 3(b), between carbon and metal atoms. The charge density difference is calculated as the charge density of the full system minus the sum of the charge densities of the metal slab and the SWNT calculated as isolated systems in the geometry positions of the optimised full system. However, the charge density difference at the interface with Au, reported

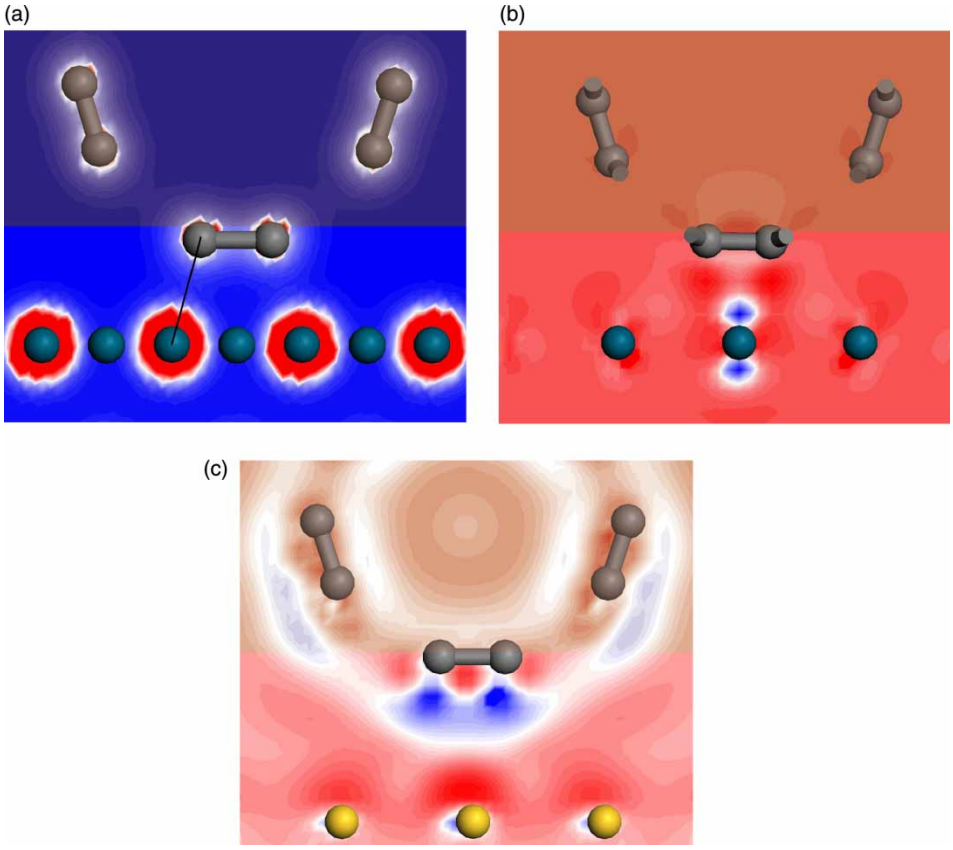


Figure 3. Planar contour maps of (a) the electrostatic potential (no barrier has been found along the black line) for the interface with palladium, (b) the charge density difference for the interface with palladium and (c) the charge density difference for the interface with gold. The mapped values are the highest (lowest) in the red (blue) regions (colour online).



in Figure 3(c), is not positive between Au and C atoms and therefore covalent bonds are not formed.

We have also optimised different starting configurations of the Au(111)–SWNT and Pd(111)–SWNT systems by rotating the SWNT along its axis. We did not find chemisorbed states for the system on the Au surface, while we have also studied for comparison of a physisorbed configuration for Pd. Indeed, in Figure 1(e),(f), we show the top view of the atom positions of chemisorbed and physisorbed SWNT in the contact zone with Pd (the first layer of the metal and the C atoms nearest to the surface) within the periodic cell. In the chemisorbed configuration, carbon atoms form a parallel $C_2$ dimer structure. Chemisorption of carbon dimers on the transition metal surface is favoured due to the presence of $\pi$-electrons that have the right symmetry to overlap with the 4d electrons and to form coordinate bonds. Consequently, a chemisorbed $C_2$ dimer has two possible positions on the surface of a transition metal, i.e. on top of the 4d metal atom or between two of them, as shown in Figure 1(e). The C atoms of the SWNT nearby metal atoms undergo a transition from $sp^2$ to $sp^3$ with the formation of covalent bonds on the surface. A zig-zag chain of carbons is the structure near the Pd surface (as shown in Figure 1(f)) for the physisorbed system that cannot coordinate to form bonds with the metal atoms. The binding energy for this structure is 0.53 eV and the distance from the slab is 2.93 Å. The average and the 'atom to atom' energy barriers are 3.4 and 3.2 eV, respectively, inferior with respect to those for the gold electrode.

We want to clarify the causes of the minor reactivity of the Au surface. Therefore, we calculated the local DOS referred to the first layer of the metal substrates as well as to the C atoms nearest to the surface, and then we have plotted the partial DOS (PDOS) in Figure 4 to resolve the contributions according to the angular momentum (i.e. s-, p- and d-symmetry type) of the states and to have qualitative information on the nature of electron hybridisation. Of course, the formation of covalent bonds is promoted when d-orbitals are contributing more to the DOS near the Fermi energy, so that $\pi$-electrons can coordinate with metal hybrid orbitals to bind the SWNT.

The PDOS of d-orbitals associated with the first layer of the palladium slab on the Fermi energy is very large compared to the PDOS of s- and p-orbitals from the metal. The PDOS related to the C atoms shows that p-orbital

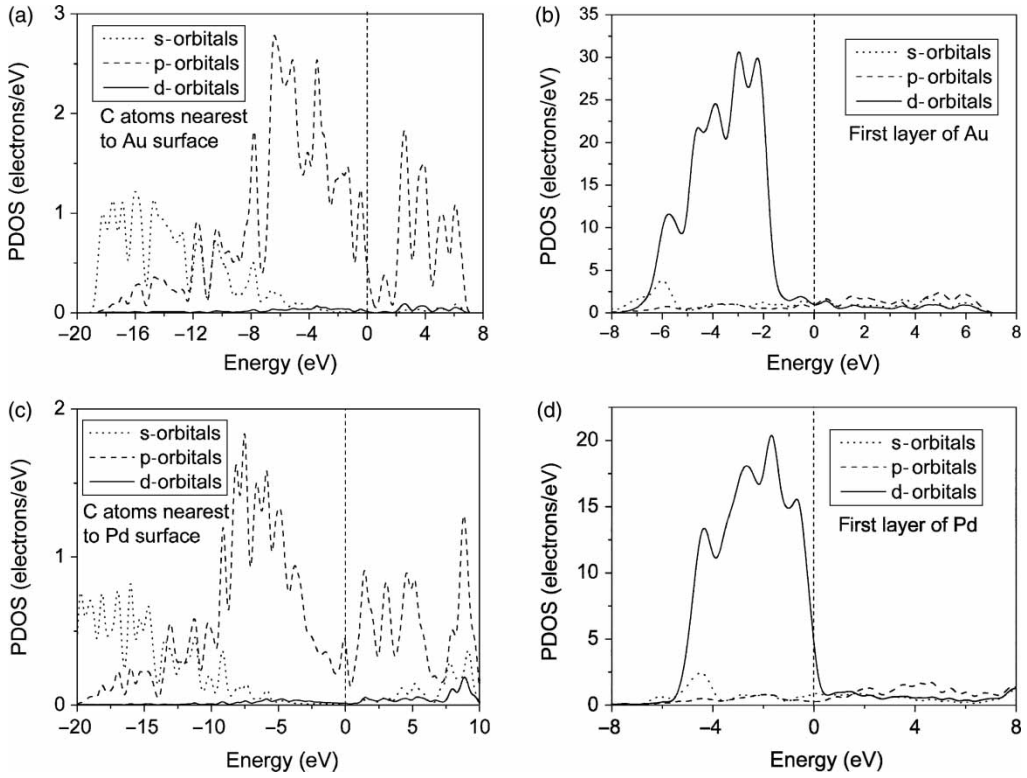


Figure 4. The PDOS for (a) the carbon atoms nearest to the gold surface, (b) the first layer of gold, (c) the carbon atoms nearest to the palladium surface and (d) the first layer of palladium. The Fermi energy has been set to 0 eV.



contributions have a peak on the Fermi energy so that carbon p-orbital are available to overlap with metal d-orbitals to share electrons and form bonds. On the contrary, the PDOS of d-orbitals for Au is very low as the nearest high peak is 2.2 eV below the Fermi energy and the covalent bond cannot be formed.

In general, it has been demonstrated [21] that the degree of orbital overlap is not the only factor controlling the strength of the adsorbate–metal interaction but also the degree of filling of the antibonding states should be taken into account. The result is that Au is more stable (less reactive) than 3d and 4d transition metals. In order to give an example of the interaction between metal atoms and carbon honeycomb structures, and to have a clear visualisation of the bonding or antibonding character of the orbitals, we also made a periodic cell model for either Au or Pd single atom adsorbed on top site (resulted to be the most stable adsorption site) in a $2 \times 2$ graphene surface with edges $a = b = 4.920$ Å. The binding energy of the Au (Pd) atom is 0.60 eV (1.10 eV) with the distance from the graphene layer of 2.29 Å (2.08 Å). We found (see Figure 5) that the HOMO of the Au–graphene system is of antibonding character, while the nearest bonding orbital is HOMO-5 for which the energy level is located 1.5 eV below HOMO. On the other hand, the HOMO-1 for the Pd–graphene system is of bonding character and is just 0.3 eV below the HOMO of antibonding character. Therefore, the Au—C bond is less stable than the Pd—C bond due to the occupation of antibonding orbitals; the same considerations can be extended to the interaction between metal surfaces and SWNTs.

We have also investigated the interface between a vertical graphene ribbon and either Au(110) or Pd(110) slab, in the geometrical arrangement reported in Figure 6, where the $C_2$ dimer at the ribbon edge is above the hollow between four metal atoms. Two periodic cells were built and the binding energies were 2.69 and 2.37 eV with graphene–slab distances of 1.250 and 1.332 Å for Au and Pd, respectively. No energy barrier was found for the average or local SCF electrostatic potential, so that we can suppose that no SB is formed for the ideal arrangement. However, these results translated to the open edge of a SWNT in the end-contact geometry state that, only when atom matching allows having $C_2$ dimers in the positions where bond coordination is possible, charge transfer between the electrode and the SWNT without any barrier is achievable. Every time the SWNT open edge does not match with the lattice of the metal surface, high energy barriers are settled. Carbon dimers at the edge of SWNTs with a large radius are more likely to match with the lattice of the metal surface so that low SBs are established at the end contact.

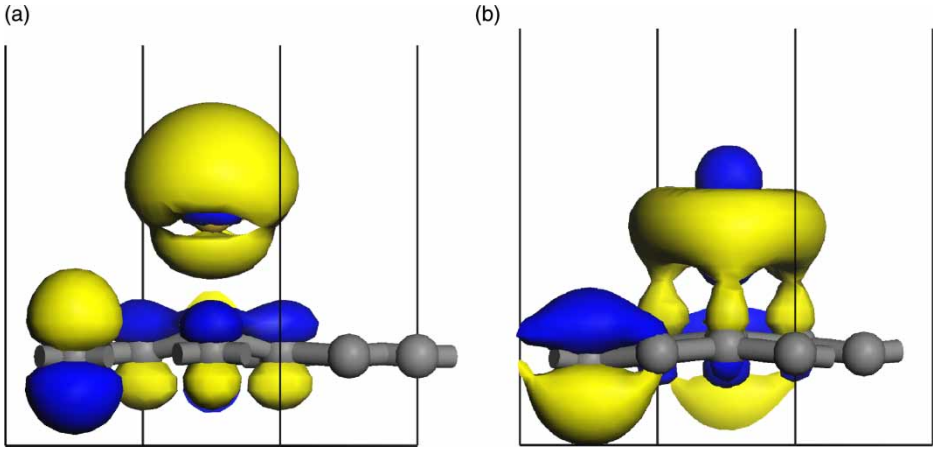


Figure 5. (a) The HOMO of the gold atom and (b) the HOMO-1 of the palladium atom adsorbed on top site of the graphene surface.

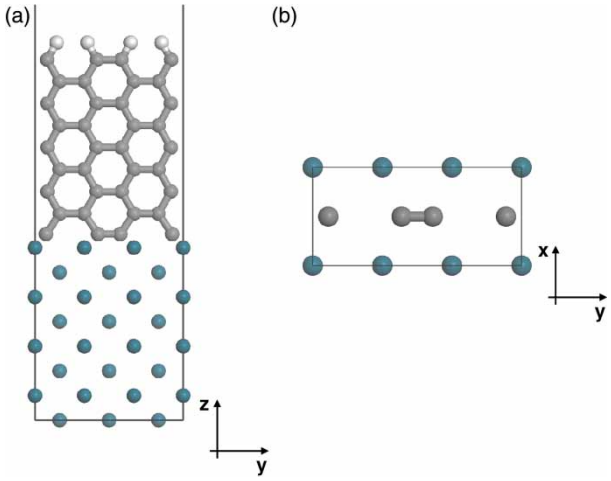


Figure 6. Atomistic periodic model after optimisation of the interface of the carbon ribbon with the palladium slab in (a) front view and (b) top view. In (b), only the first-layer metal atoms and bottom carbon dimers are shown.

## 4. Conclusions

The different behaviours of Au and Pd surfaces with respect to the side-wall adsorption of the SWNT can be understood in terms of the PDOS analysis at the interface. The Au–SWNT interaction is weak so that the SWNT can only be physisorbed, and we have related this behaviour to the low density of metal d-states at the Fermi energy. We observed that orbitals of d-symmetry type are essential in order to have orbital overlapping with carbon $\pi$-electrons and bond formation. Indeed, stronger interaction has been found for the Pd–SWNT interface where the DOS has large contributions from d-orbitals so that stable covalent bonds are formed. However, we have shown that the degree of filling of the antibonding states also plays a key role in controlling the strength of the adsorbate–metal interaction. Indeed, the simulations for the single atom adsorbed on the graphene surface demonstrated that the binding energy of the Au atom is much lower than that of Pd atom and the weakness of the covalent bond is related to the antibonding character of the HOMO. In order to evaluate the quality of the generic metal–CNT contact, other factors should also be taken into account, such as the wetting capability and the chemical reactivity of the metal.

We have also modelled the end-contact geometry and found that the correct matching for $C_2$ dimers is easier when SWNTs with a large diameter are involved. We can conclude that, in addition to the smaller energy gap, this is another reason that makes lower the SB of SWNTs with a large diameter.

The analysis carried out in the present work can be useful to drive the design of devices based on CNTs in which the SB dominates the electrical behaviour or where ohmic contacts are required, as for interconnects.

## References

[1] S.J. Tans, A.R.M. Verschueren, and C. Dekker, *Room-temperature transistor based on a single carbon nanotube*, Nature 393 (1998), pp. 49–52.
[2] H.W.C. Postma, T. Teepen, Z. Yao, M. Grifoni, and C. Dekker, *Carbon nanotube single-electron transistors at room temperature*, Science 293 (2001), pp. 76–79.
[3] R. Martel, T. Schmidt, H. Shea, T. Hertel, and P. Avouris, *Single- and multi-wall carbon nanotube field-effect transistors*, Appl. Phys. Lett. 73 (1998), pp. 2447–2449.
[4] D. Normile, *Nanotubes generate full-color displays*, Science 286 (1999), pp. 2056–2057.
[5] S.J. Tans, M.H. Devoret, H. Dai, A. Thess, R.E. Smalley, L.J. Geerligs, and C. Dekker, *Individual single-wall nanotubes as quantum wires*, Nature 386 (1997), pp. 474–477.
[6] M. Bockrath, D.H. Cobden, P.L. McEuen, N.G. Chopra, A.Z.A. Thess, and R.E. Smalley, *Single-electron transport in ropes of carbon nanotubes*, Science 275 (1997), pp. 1922–1925.
[7] P.G. Collins, K. Bradley, M. Ishigami, and A. Zettl, *Extreme oxygen sensitivity of electronic properties of carbon nanotubes*, Science 287 (2000), pp. 1801–1804.
[8] V. Derycke, R. Martel, J. Appenzeller, and P. Avouris, *Controlling doping and carrier injection in carbon nanotube transistors*, Appl. Phys. Lett. 80 (2002), pp. 2773–2775.

[9] S. Heinze, M. Radosavljevic, J. Tersoff, and P. Avouris, *Unexpected scaling performance of carbon nanotube transistors*, Phys. Rev. B 68 (2003), pp. 235418-1–235418-5.
[10] A.P. Graham, G.S. Duesberg, R. Seidel, M. Liebau, E. Unger, F. Kreupl, and W. Hönlein, *Towards the integration of carbon nanotubes in microelectronics*, Diamond Relat. Mater. 13 (2004), pp. 1296–1300.
[11] Z. Chen, J. Appenzeller, J. Knoch, Y.M. Lin, and P. Avouris, *The role of metal–nanotube contacts in the performance of CNTFETs*, Nano Lett. 5 (2005), pp. 1497–1502.
[12] B. Shan and K. Cho, Ab initio *study of Schottky barriers at metal–nanotube contacts*, Phys. Rev. B 70 (2004), pp. 233405-1–233405-4.
[13] S. Dag, O. Gülseren, S. Ciraci, and T. Yildirim, *Electronic structure of the contact between carbon nanotube and metal electrodes*, Appl. Phys. Lett. 83 (2003), pp. 3180–3182.
[14] A. Maiti and A. Ricca, *Metal–nanotube interactions – Binding energies and wetting properties*, Chem. Phys. Lett. 395 (2004), pp. 7–11.
[15] P. Bai, E. Li, K.T. Lam, O. Kurniawan, and W.S. Koh, *Carbon nanotube Schottky diode: An atomic perspective*, Nanotechnology 19 (2008), pp. 115203-1–115203-6.
[16] W. Zhu and E. Kaxiras, *The nature of contact between Pd leads and semiconducting carbon nanotubes*, Nano Lett. 6 (2006), pp. 1415–1418.
[17] V. Vitale, A. Curioni, and W. Andreoni, *Metal–carbon nanotube contacts: The link between Schottky barrier and chemical bonding*, J. Am. Chem. Soc. 130 (2008), pp. 5848–5849.
[18] B. Delley, *An all-electron numerical method for solving the local density functional for polyatomic molecules*, J. Chem. Phys. 92 (1990), pp. 508–517.
[19] B. Delley, *From molecules to solids with the DMol$^3$ approach*, J. Chem. Phys. 113 (2000), pp. 7756–7764.
[20] B. Delley, *Hardness conserving semilocal pseudopotentials*, Phys. Rev. B 66 (2002), pp. 155125-1–155125-9.
[21] B. Hammer and J.K. Nørskov, *Why gold is the noblest of all the metals*, Nature 376 (1995), pp. 238–240.